Pergamon

Solid State Communications, Vol. 105, No. 3, pp. 161–164, 1998

0038–1098/98 $19.00+.00

PII: S0038-1098(97)10087-4

ELECTRONIC EXCITATIONS OF AN ELECTRON-GAS CYLINDER BUNDLE

M.F. Lin,[a] C.S. Huang[b] and D.S. Chuu[b]

[a]Department of Physics, National Cheng Kung University, Tainan 70101, Taiwan, The Republic of China
[b]Electrophysics Department, National Chiao Tung University, Hsinchu 30050, Taiwan, The Republic of China

(*Received* 20 *August* 1997; *accepted* 24 *September* 1997 *by S. Ushioda*)

We study the dielectric response function of an electron-gas cylinder bundle. The electron–electron interactions among different cylinders are taken into account. The electronic excitations are associated with those of an isolated cylinder. However, a cylinder bundle exhibits the three-dimensional characteristics, but a single cylinder the one-dimensional characteristics. The excitation properties are highly anisotropic. The plasma oscillations perpendicular and parallel to the axial direction quite differs from each other. The ratio between their oscillation frequencies is generally smaller than $1/\sqrt{2}$, which depends on the cylinder radius and the effective mass. © 1997 Elsevier Science Ltd

Keywords: D. dielectric response, D. electron–electron interactions.

A cylinder bundle, which is made up of the identical hollow cylinders, could form a two-dimensional (2D) lattice, e.g. a triangular lattice (Fig. 1). An isolated cylinder is a mesoscopic metal tube [1] or a carbon nanotube [2]. The metallic carbon nanotube bundle was recently reported by Thess *et al.* [3]. The objective of this work is to investigate the electronic excitations of the cylinder bundles by evaluating their dielectric function ϵ.

Here the charge carriers confined on a hollow cylinder are modelled as an electron gas (EGS) [1, 4–7]. The eigenstates are

$$\Psi_\beta(r_\perp, \phi, z) = e^{ikz}\, e^{il\phi}\delta(r_\perp - a)/\sqrt{r_\perp}, \tag{1}$$

and the eigenvalues are

$$E_\beta = k^2/2m^* + l^2/2m^*a^2, \tag{2}$$

where $|\beta\rangle = |k, l\rangle$. k is the wave vector along the axial direction, l the angular momentum or the subband index, m^* the effective mass and a the cylinder radius. Due to the cylindrical symmetry, the transferred momentum (q) and angular momentum (L) are conserved in the electron–electron (e–e) interactions. Hence each EGS cylinder exhibits the L-decoupled electronic excitations, with the strong q-dependence [4–7].

The Bloch functions of a cylinder bundle, which have the 2D lattice vector $\mathbf{R}_{\perp,n}$, are expressed by

$$|\alpha\rangle|\mathbf{k}_\perp, \beta\rangle = C\sum_{\mathbf{R}_{\perp,n}} \exp(i\mathbf{k}_\perp \cdot \mathbf{R}_{\perp,n})\Psi_\beta(\mathbf{r}_\perp - \mathbf{R}_{\perp,n}, z). \tag{3}$$

C is the normalization factor. $\perp$ denotes the vector perpendicular to the axial direction. For example, $\mathbf{k}_\perp$ is perpendicular to k. The cylinder bundle is assumed to be perturbed by an external potential $V^{ex}(\mathbf{q}_\perp, q, w)$. It would induce charge fluctuations on all cylinders. The induced potential due to the screening charges could be obtained from the Poisson's equation

$$V^{in}(\mathbf{q}_\perp, q, w) = V(\mathbf{q}_\perp, q)n^{in}(\mathbf{q}_\perp, q, w). \tag{4}$$

$V(\mathbf{q}_\perp, q) = 4\pi e^2/(q_\perp^2 + q^2)$ is the Coulomb interaction of a 3D EGS. The e–e interaction has changed from the 1D [4–7] to the 3D form, when the quasi-1D cylinders are packed into the crystalline bundle.

The approximation, which is similar to the self-consistent-field approach [8], is used to calculate the induced charge density (n^{in}). Within the linear response approximation, we obtain

$$n^{in}(\mathbf{q}_t, w) = 2\sum_{\alpha,\alpha',\mathbf{q}'_t} V^{eff}(\mathbf{q}'_t, w)\langle\alpha'|e^{i\mathbf{q}'_t\cdot\mathbf{r}}|\alpha\rangle\langle\alpha|e^{-i\mathbf{q}_t\cdot\mathbf{r}}|\alpha'\rangle \times \frac{f^0(E_{\alpha'}) - f^0(E_\alpha)}{E_{\alpha'} - E_\alpha - (w + i\delta)}, \tag{5}$$

where $\mathbf{q}_t = (\mathbf{q}_\perp, q)$. The factor of 2 accounts for the spin degeneracy. $V^{eff} = V^{ex} + V^{in}$ is the effective potential. f^0 is the Fermi–Dirac function. The many-body effects due to exchange-correlation holes are neglected within the linear response. As a result of the periodicity of the Bloch functions, the matrix elements in equation (5) is

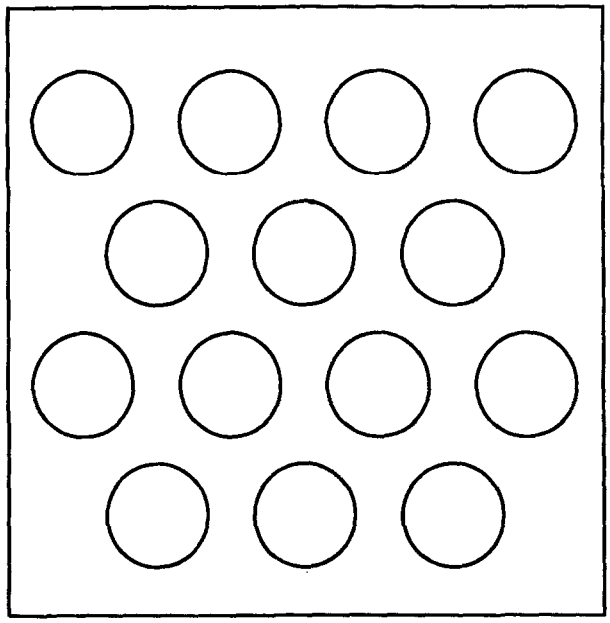

Fig. 1. The hollow cylinders are packed into a two-dimensional triangular lattice.

further reduced to

$$\langle\alpha'|e^{i\mathbf{q}'_\perp\cdot\mathbf{r}}|\alpha\rangle = \delta(\mathbf{k}'_\perp - \mathbf{k}_\perp - \mathbf{q}'_\perp - \mathbf{G}'_n)\delta(k' - k - q) \times M_L(\mathbf{q}'_\perp), \tag{6a}$$

where

$$M_L(\mathbf{q}'_\perp) = \int d\mathbf{r}_\perp e^{i\mathbf{q}'_\perp\cdot\mathbf{r}_\perp}\Psi^*_{l'}(r_\perp,\phi)\Psi_l(r_\perp,\phi) = \int_0^{2\pi} e^{-iL\phi}\, e^{iq'_x a\cos\phi}\, e^{iq'_y a\sin\phi}\, d\phi. \tag{6b}$$

$(q'_x, q'_y) = \mathbf{q}'_\perp$. $\mathbf{G}_n$ is a 2D reciprocal-lattice vector. The effects from the Umklapp scattering are included in equation (6a). M_L, which is derived from the e–e interactions of Bloch states, only depends on the difference of angular momentum $L = l - l'$. This result clearly illustrates that the dielectric response of a cylinder bundle is associated with the various L's excitations of separate hollow cylinders.

The effective potential obtained from equations (4)–(6) is

$$V^{eff}(\mathbf{q}_\perp + \mathbf{G}_n, q, w) = V^{ex}(\mathbf{q}_\perp + \mathbf{G}_n, q, w) + V^{in}(\mathbf{q}_\perp + \mathbf{G}_n, q, w), \tag{7a}$$

and

$$V^{in}(\mathbf{q}_\perp + \mathbf{G}_n, q, w) = V(\mathbf{q}_\perp + \mathbf{G}_n, q)\sum_{\mathbf{G}_{n'}}\sum_L \times M^*_L(\mathbf{q}_\perp + \mathbf{G}_n)M_L(\mathbf{q}_\perp + \mathbf{G}_{n'}) \times V^{eff}(\mathbf{q}_\perp + \mathbf{G}_{n'}, q, w)\chi_L(q, w), \tag{7b}$$

where

$$\chi_L(q, w) = \frac{2N_A}{(2\pi)^2}\sum_l \times \int dk \frac{f^0[E(k+q, l+L)] - f^0[E(k,l)]}{E(k+q, l+L) - E(k,l) - (w + i\delta)}. \tag{7c}$$

$\mathbf{q}_\perp$ in equation (7a) is confined within the first Brillouin zone. $\chi_L(q, w)$ is the response function of an isolated cylinder [4–7]. N_A is the cylinder number per area. The dielectric function, which satisfies $[\epsilon]V^{eff} = V^{ex}$, is

$$[\epsilon]_{\mathbf{G}_n,\mathbf{G}_{n'}}(\mathbf{q}_\perp, q, w) = \epsilon_0\delta_{\mathbf{G}_n\mathbf{G}_{n'}} - V(\mathbf{q}_\perp + \mathbf{G}_n, q)\sum_L M^*_L \times (\mathbf{q}_\perp + \mathbf{G}_n)M_L(\mathbf{q}_\perp + \mathbf{G}_{n'})\chi_L(q, w), \tag{8}$$

where ϵ_0 is the background dielectric constant. $[\epsilon]$ in equation (8) remains the similar form, when each cylinder is threaded by a uniform magnetic flux ϕ_m. It only needs to change $\chi_L(q, w)$ into $\chi_L(q, w, \phi_m)$ [4].

The dielectric function in equation (8) is an $n \times n$ matrix. The term $\mathbf{G}_n = \mathbf{G}_{n'} = 0$ is mainly related to the intensity of the excitation spectrum. The following calculations are mainly focused on

$$[\epsilon]_{0,0} = \epsilon_0 - V(\mathbf{q}_\perp, q)\sum_L \chi_L(q, w)|M_L(\mathbf{q}_\perp)|^2. \tag{9}$$

$M_L(\mathbf{q}_\perp)$ in equation (6b) could be evaluated from the series expansion of $\exp(i\mathbf{q}_\perp\cdot r_\perp)$. By the detailed analysis, $[\epsilon]_{0,0}$ is approximately given by

$$[\epsilon]_{0,0} \approx \epsilon_0 - \frac{8\pi^2e^2}{(q_\perp^2 + q^2)}\left\{\left[1 + \frac{a^4q_\perp^4}{16} + \frac{a^8q_\perp^8}{4096}\right]\chi_{L=0}(q, w) + \left[\frac{a^2q_\perp^2}{2} + \frac{a^6q_\perp^6}{128}\right]\chi_{L=1}(q, w) + \left[\frac{a^4q_\perp^4}{32} + \frac{a^8q_\perp^8}{4608}\right]\chi_{L=2}(q, w) + \frac{a^6q_\perp^6}{1152}\chi_{L=3}(q, w)\right\}. \tag{10}$$

The approximate expression in equation (10) is good at $aq_\perp \leq 3$. The dielectric function markedly depends on the direction and the magnitude of $\mathbf{q}_t$. The angle between $\mathbf{q}_t$ and the axial direction is characterized by θ. Hence the excitation spectrum ($\mathrm{Im}\{-1/[\epsilon]_{0,0}\}$) of a cylinder bundle would exhibit the highly anisotropic behavior.

The two simple cases, $\mathbf{q}_\perp = 0$ and $q = 0$, are discussed. The dielectric function in the absence of $\mathbf{q}_\perp$ ($\theta = 0$) is

$$[\epsilon]_{0,0}(q, w) = \epsilon_0 - \frac{8\pi^2 e^2}{q^2}\chi_{L=0}(q, w). \tag{11}$$

The response function of a cylinder bundle is indicated to be the superposition of the $L = 0$ excitations of all cylinders, if the external electric field is parallel to the axial direction. The dielectric function in equation (11) is similar to that of an isolated cylinder. However, the Coulomb interaction of the former belongs to the 3D form and the latter the 1D form [4–7]. The excitation properties of a cylinder bundle, e.g. plasmons, should contrast greatly with those of a single cylinder. The plasmon frequency w_p could be obtained from $\mathrm{Re}[\epsilon]_{0,0} = 0$. $w_p(\theta = 0°, q \to 0) = \sqrt{4\pi N e^2/\epsilon_0 m^*}$ at long-wavelength limit, since $\chi_{L=0}(q \to 0, w) = a n_e N_A q^2/m^* w^2$ [4]. n_e is the carrier number per area in each cylinder and N is the total carrier number per volume. This result is similar to that of a 3D EGS. Hence the plasma oscillations along the tube axis are suggested to behave as that of a 3D EGS. This plasmon belongs to an optical plasmon, which is completely different from the 1D acoustic plasmon (the $L = 0$ mode) in a single cylinder [4–7]. That the thorough change of the e–e interactions is the main reason.

For the $q = 0$ case ($\theta = 90°$), the dielectric function at small $\mathbf{q}_\perp$ is

$$[\epsilon]_{0,0}(\mathbf{q}_\perp, w) \approx \epsilon_0 - 4\pi^2 e^2 a^2 \chi_{L=1}(q = 0, w) - \frac{\pi^2 e^2 a^4 q_\perp^2}{4}\chi_{L=2}(q = 0, w). \tag{12}$$

The dielectric response at long-wavelength limit ($\mathbf{q}_\perp \to 0$) mainly comes from the superposition of the $L = 1$ excitations, which quite differs from that in the case of $\mathbf{q}_\perp = 0$ [equation (11)]. This result further illustrates that the cylinder bundle owns the highly anisotropic characteristics. If the plasmon frequency is much higher than the single-particle excitation energy ($|E(k = q, l + 1) - E(k, l)|$), $\chi_{L=1}(q = 0, w) = n_e N_A/m^* w^2$ [4]. Under such a condition, the plasmon frequency at long-wavelength limit is $w_p(\theta = 90°, \mathbf{q}_\perp \to 0) = \sqrt{2\pi N e^2/\epsilon_0 m^*}$. Moreover, there is a special ratio $1/\sqrt{2}$ between the plasmon frequencies for the plasma oscillations perpendicular and parallel to the axial direction. In addition, a similar ratio $1/\sqrt{2}$ could also be found in the relation between the surface plasmon and the bulk plasmon of normal metals. In general, the ratio $w_p(\theta = 90°, \mathbf{q}_\perp \to 0)/w_p(\theta = 0°, q \to 0)$, as shown in Fig. 2, is smaller than $1/\sqrt{2}$. It depends on the nanotube radius and the effective mass. The plasmon in the $q = 0$ or $\mathbf{q}_\perp = 0$ case belongs to an optical plasmon, which implies that the charge carriers in a cylinder bundle would behave as a 3D EGS for any $\mathbf{q}_t$.

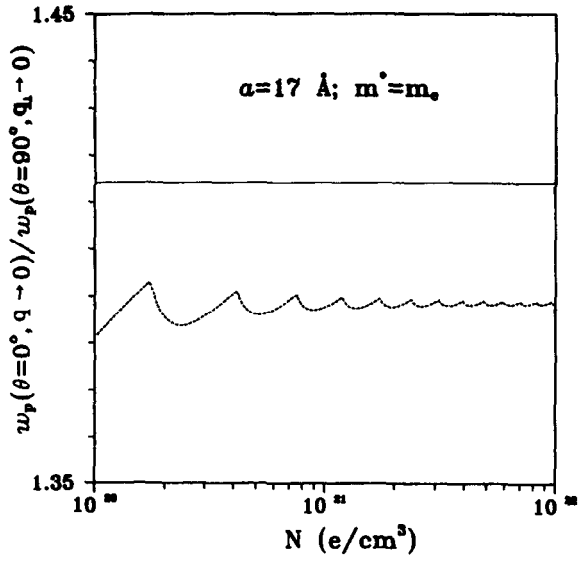

Fig. 2. The ratio between the long-wavelength plasmon frequencies for the plasma oscillations perpendicular and parallel to the axial direction. It is shown as a function of the total carrier density at $a = 17$ Å and $m^* = m_e$.

In short, we have calculated the dielectric function of an electron-gas cylinder bundle. It could be further used to study the excitation properties of metal tube bundles [1] and carbon nanotube bundles [3]. For example, the electron-gas cylinder bundle is suitable in understanding the collective excitations of the conduction electrons in the intercalated carbon nanotube bundles [9, 10]. The details will be studied elsewhere. The cylinder bundles would exhibit the highly anisotropic behavior and the three-dimensional characteristics. The plasma oscillations perpendicular and parallel to the nanotube axis are very different from each other. The ratio between their oscillation frequencies is generally smaller than $1/\sqrt{2}$, which depends on the nanotube radius and the effective mass.

Acknowledgements—This work was supported in part by the National Science Council of Taiwan, Republic of China under the Grant No. NSC 86-2112-M-009-006.

REFERENCES

1. Cheung, H., Riedel, E.K. and Gefen, Y., *Phys. Rev. Lett.*, **62**, 1989, 587; *IBM J. Res. Develop.*, **32**, 1988, 359.
2. Iijima, S., *Nature*, **354**, 1991, 56.
3. Thess, A. *et al.*, *Science*, **273**, 1996, 483.
4. Lin, M.F. and Shung, K.W.-K., *Phys. Rev.*, **B47**, 1993, 6617; **B48**, 1993, 5567.

5. Longe, P. and Bose, S.M., *Phys. Rev.*, **B48,** 1993, 18239.
6. Yannouleas, C., Bogachek, E.N. and Landman, U., *Phys. Rev.*, **B50,** 1994, 7977.
7. Sato, O., Tanaka, Y., Kobayashi, M. and Hasegawa, A., *Phys. Rev.*, **B48,** 1993, 1947.
8. Ehrenreich, H. and Cohen, M.H., *Phys. Rev.*, **115,** 1959, 786.
9. Lee, R.S., Kim, H.J., Fischer, J.E., Thess, A. and Smalley, R.S., *Nature*, **388,** 1997, 255.
10. Rao, A.M., Eklund, P.C., Bandow, S., Thess, A. and Smalley, R.S., *Nature*, **388,** 1997, 257.